

# The Influence of 13-*cis* Retinoic Acid on Human Meibomian Gland Epithelial Cells

Juan Ding, Wendy R. Kam, Julia Dieckow, and David A. Sullivan

Schepens Eye Research Institute, Massachusetts Eye and Ear, Department of Ophthalmology, Harvard Medical School, Boston, Massachusetts

Corresponding authors: Juan Ding, Schepens Eye Research Institute, 20 Staniford Street, Boston, MA 02114; juan\_ding@meei.harvard.edu. David A. Sullivan, Schepens Eye Research Institute, 20 Staniford Street, Boston, MA 02114; david.sullivan@schepens.harvard.edu.

Submitted: February 13, 2013

Accepted: May 22, 2013

Citation: Ding J, Kam WR, Dieckow J, Sullivan DA. The influence of 13-*cis* retinoic acid on human meibomian gland epithelial cells. *Invest Ophthalmol Vis Sci*. 2013;54:4341–4350. DOI:10.1167/iovs.13-11863

**PURPOSE.** Meibomian gland dysfunction (MGD) is a primary cause of dry eye disease. One of the risk factors for MGD is exposure to 13-*cis* retinoic acid (13-*cis* RA), a metabolite of vitamin A. However, the mechanism is not well understood. We hypothesize that 13-*cis* RA inhibits cell proliferation, promotes cell death, alters gene and protein expressions, and attenuates cell survival pathways in human meibomian gland epithelial cells.

**METHODS.** To test our hypotheses, immortalized human meibomian gland epithelial cells were cultured with or without 13-*cis* RA for varying doses and time. Cell proliferation, cell death, gene expression, and proteins involved in proliferation/survival and inflammation were evaluated.

**RESULTS.** We found that 13-*cis* RA inhibited cell proliferation, induced cell death, and significantly altered the expression of 6726 genes, including those involved in cell proliferation, cell death, differentiation, keratinization, and inflammation, in human meibomian gland epithelial cells. Further, 13-*cis* RA also reduced the phosphorylation of Akt and increased the generation of interleukin-1 $\beta$  and matrix metalloproteinase 9.

**CONCLUSIONS.** Exposure to 13-*cis* RA inhibits cell proliferation, increases cell death, alters gene expression, changes signaling pathways, and promotes inflammatory mediator and protease expression in meibomian gland epithelial cells. These effects may be responsible, at least in part, for the 13-*cis* RA-related induction of MGD.

Keywords: retinoic acid, meibomian gland dysfunction, dry eye disease

Meibomian glands play a critical role in the health and well-being of the ocular surface.<sup>1,2</sup> These glands secrete a lipid and protein mixture that provides a clear optical surface for the cornea, interferes with bacterial colonization, and retards tear overflow.<sup>1,2</sup> These glandular secretions also promote stability and prevent evaporation of the tear film.<sup>1,2</sup> Conversely, meibomian gland dysfunction (MGD) destabilizes the tear film, increases its evaporation and osmolarity, and is believed to be the major cause of dry eye disease in the world.<sup>1-5</sup>

The most common form of MGD is terminal excretory duct obstruction, due to hyperkeratinization of the ductal epithelium and an increased viscosity of meibum.<sup>1</sup> This obstruction, which is commonly found during aging and androgen deficiency,<sup>1,6</sup> may lead to cystic dilatation of glandular ducts, acinar cell atrophy, and a loss of secretory epithelial cells (i.e., meibocytes).<sup>1</sup> The MGD may also facilitate bacterial growth on the lid margin and promote inflammation in the adjacent conjunctiva (e.g., posterior blepharitis).<sup>1</sup>

Aside from aging and androgen insufficiency, another significant risk factor for the development of MGD is exposure to 13-*cis* retinoic acid (13-*cis* RA, or isotretinoin).<sup>1,6</sup> This compound, which originates from vitamin A, causes the following meibomian gland sequelae: ductal keratinization, acinar cell degeneration, periacinar fibrosis, glandular atrophy, and reduced and abnormal secretions.<sup>1</sup> Further, 13-*cis* RA exposure is associated with tear film instability and hyperosmolarity, dry eye symptoms, and blepharitis.<sup>1</sup> In effect, the

retinoic acid derivatives promote MGD and evaporative dry eye.<sup>1</sup>

These effects of 13-*cis* RA on the meibomian gland are not surprising. This agent (first marketed as Accutane [isotretinoin] by F. Hoffmann–La Roche Ltd., Basel, Switzerland) is frequently used for the dermatologic treatment of severe acne, because it significantly decreases the growth, development, and lipid production of sebaceous gland epithelial cells (sebocytes).<sup>7,8</sup> Given that the meibomian gland is a large sebaceous gland, it is not surprising that 13-*cis* RA exerts an analogous impact on this tissue. However, the influence of 13-*cis* RA may become an even greater health problem in the near future. The reason is that RA, which is converted to all-*trans* retinoic acid in sebocytes,<sup>9</sup> is the key ingredient of antiaging cosmetics. These skin creams are commonly sold for use around the eyelids and could promote the development of MGD in a population (i.e., aged) known to be very susceptible to the development of dry eye.<sup>10</sup> Indeed, this antiaging cosmetic use could become a significant challenge to the effective treatment of dry eye disease, given that approximately 25% of the US population will be 65 years of age and older by the year 2050.

The mechanism(s) by which 13-*cis* RA induces MGD is unknown. It has been shown that 13-*cis* RA causes alterations in sebocyte gene expression, decreases basal sebocyte proliferation, prohibits sebocyte terminal differentiation, induces sebocyte apoptosis, and suppresses sebum production up to 90%.<sup>8,11</sup> We hypothesize that retinoic acid derivatives act on the meibomian gland in a manner analogous to that of the

sebaceous gland. More specifically, we hypothesize that 13-*cis* RA inhibits cell proliferation, promotes cell death, alters gene and protein expressions, and attenuates cell survival pathways in human meibomian gland epithelial cells. We propose to test these hypotheses in the current study.

## MATERIALS AND METHODS

### Cell Culture and Treatment

Immortalized human meibomian gland epithelial cells<sup>12</sup> were maintained in keratinocyte serum-free medium (KSFM) supplemented with 5 ng/mL epidermal growth factor (EGF) and 50 µg/mL bovine pituitary extract (BPE; Invitrogen Corp., Carlsbad, CA) as previously described.<sup>13</sup> Immortalized human conjunctival cells (gift of Ilene Gipson, Schepens Eye Research Institute, Boston, MA) were maintained in KSFM supplemented with 5 ng/mL EGF and 25 µg/mL BPE. 13-*cis* Retinoic acid (13-*cis* RA; Sigma-Aldrich, St. Louis, MO) was reconstituted in 100% ethanol to 10 mM and stored under argon gas at -20°C, protected from light. All procedures involving RA were performed under dim yellow light.

### Cell Proliferation Assay

To assess cell proliferation in response to 13-*cis* RA, 40,000 or 20,000 cells were seeded in 6- or 12-well plates (Corning Inc., Corning, NY), respectively, and treated with or without varying doses of 13-*cis* RA for times specified. Following treatment, cells were trypsinized and counted manually using a hemocytometer (Bright-Line; American Optical Corporation, Buffalo, NY). For the WST-1 assay (Roche Diagnostics, Indianapolis, IN), cells were plated in 96-well plates and assessed according to the manufacturer's instructions. Each assay was repeated in at least three independent experiments.

### Terminal Deoxynucleotidyl Transferase dUTP Nick-End Labeling (TUNEL) Staining

To assay for apoptosis, cells were grown on four-well chamber slides (Lab-Tek II; Thermo Fisher Scientific, Rockford, IL) and exposed to 13-*cis* RA for 4 days. Samples were processed using a commercial cell death detection kit (In Situ Cell Death Detection Kit; Roche Diagnostics), following the manufacturer's instructions. Labeled dUTP alone without deoxynucleotidyl transferase was used as a negative control and DNase-I-treated cells served as positive controls. Fluorescent images were captured with commercial software (Advanced Software, version 4.0.9; SPOT Imaging Solutions, division of Diagnostic Instruments, Inc., Sterling Heights, MI) on a brightfield and epifluorescence microscope (Nikon Eclipse E800; Nikon Instruments, Inc., Melville, NY).

### Annexin V/Propidium Iodide (PI) Flow Cytometric Analysis

To quantify the cell death event, flow cytometric analysis was performed on cells labeled with Annexin V and PI. Cells were treated with varying doses of 13-*cis* RA in six-well plates for 24 hours. Staurosporin (Sigma-Aldrich) was used to induce apoptosis and hydrogen peroxide (CVS Pharmacy, Woonsocket, RI) to induce necrosis. Samples were collected and stained with Annexin V and PI using a commercial kit (ApopNexin FITC Apoptosis Detection Kit; Chemicon International, Temecula, CA), according to the manufacturer's instructions. For each sample, 300,000 events were collected. Data were analyzed using commercial software (Summit Software, v4.3;

Beckman Coulter, Inc., Fullerton, CA) and percentages of cells in early apoptosis and late apoptosis/necrosis were compared using one-way ANOVA followed by Fisher's protected least significant difference (PLSD).

### Microarray Gene Expression Analysis

Microarray gene expression analysis was performed to identify specific genes and pathways in meibomian gland cells that are affected by exposure to 13-*cis* RA. Cells were treated with 2 µM 13-*cis* RA or ethanol control for 4 days and total RNA was extracted using a commercial kit (RNeasy Mini Kit; Qiagen, Inc., Valencia, CA), according to the manufacturer's instructions. The RNA concentrations and 260/280 nm ratios were determined using a spectrophotometer (NanoDrop 1000; Thermo Scientific, Waltham, MA). RNA integrity was analyzed using commercial RNA bioanalyzer (RNA Nano 6000 Series II Chip with a Bioanalyzer 2100; Agilent Technologies, Palo Alto, CA). The RNA samples were processed commercially (Asuragen, Austin, TX) for quantitation of mRNA levels using microarray expression analysis (HumanHT-12 v.4 Expression BeadChips; Illumina, San Diego, CA), as described previously.<sup>14</sup>

Background subtracted, cubic spline normalized, nonlog-transformed data were evaluated with commercial software (available in the public domain at GeneSifter.net; Geospiza, Seattle, WA). Standardized hybridization intensity values were adjusted by adding a constant, such that the lowest intensity value for any sample equaled 16.<sup>15</sup> Gene expression data were analyzed with Student's *t*-test (two-tailed, unpaired). All data are accessible for download through the National Center for Biotechnology Information's Gene Expression Omnibus (available in the public domain at <http://www.ncbi.nlm.nih.gov/geo>) via series accession number GSE37089.

### SDS-PAGE and Immunoblots

To further investigate the gene expression array data, protein levels were studied using immunoblotting. Following treatment with 1 µM 13-*cis* RA or ethanol, cells were directly lysed in SDS sample buffer (Bio-Rad, Hercules, CA) supplemented with 1% protease inhibitor cocktail (Sigma-Aldrich) and 5% beta-mercaptoethanol (Sigma-Aldrich). Lysates were heated at 95°C for 10 minutes, separated by SDS-PAGE on 4%–20% Tris-glycine precast gels (Invitrogen Corp.), and transferred to polyvinylidene difluoride membranes. Monoclonal antibodies specific for phospho-AKT (Ser473; Cell Signaling Technology, Inc., Danvers, MA), pan-AKT (Cell Signaling Technology, Inc.), interleukin-1β (IL-1β, provided by National Cancer Institute, Bethesda, MD), matrix metalloproteinase-9 (MMP-9; Abcam, Cambridge, MA), and β-actin (Cell Signaling Technology, Inc.) were used. For phospho-AKT and IL-1β, membranes were blocked with 5% bovine serum albumin in Tris-buffered saline containing 0.1% Tween-20 (TBS/T); for all other antibodies, membranes were blocked with 5% nonfat dry milk in TBS/T. All primary antibodies were diluted 1:1000 in blocking buffer except for β-actin (1:5000). Horseradish peroxidase-conjugated secondary antibodies were goat antirabbit IgG and Fc-specific goat antimouse IgG (Sigma-Aldrich). Proteins were visualized with commercial Western blotting substrate (Pierce ECL Western Blotting Substrate; Thermo Fisher Scientific).

### Zymography for MMP-9

Gelatinase activity due to MMP-9 in the culture media was assessed by gelatin zymography. Supernatants were separated by SDS-PAGE on 7.5% acrylamide gels containing 1 mg/mL gelatin, with MMP control-6 (Sigma-Aldrich) as a positive control. To remove SDS and reveal enzyme activity, gels were

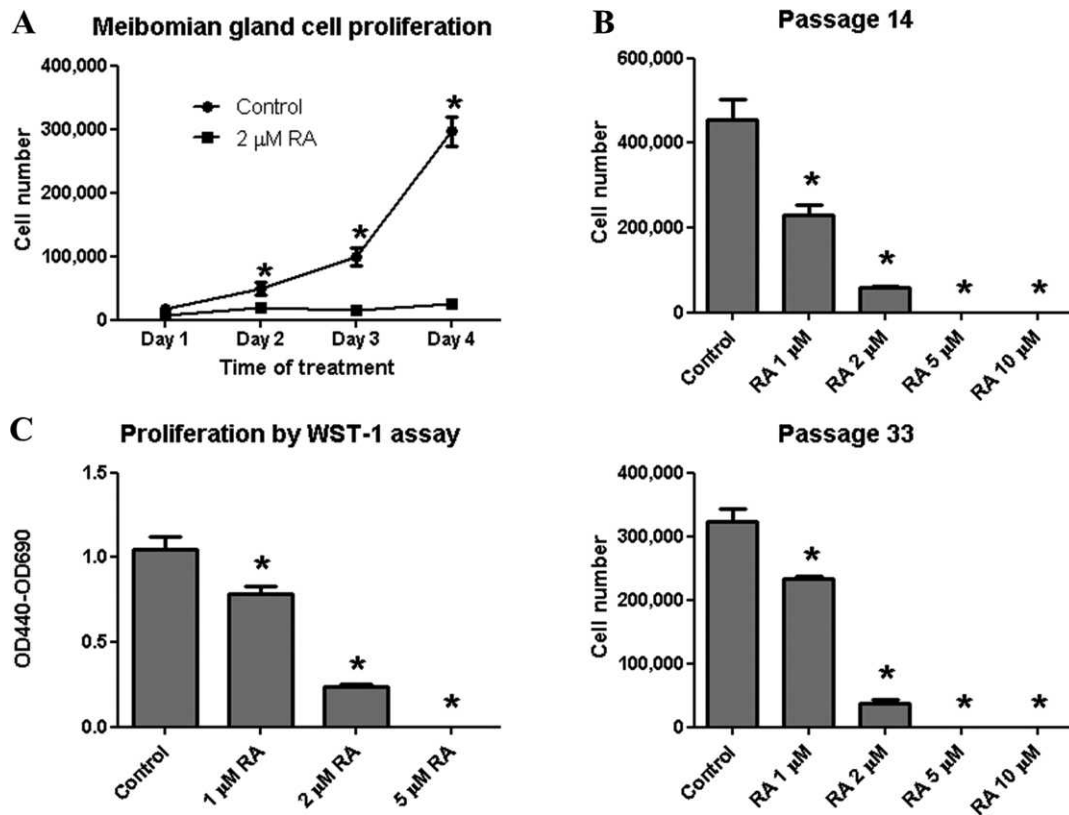


**FIGURE 1.** 13-*cis* RA inhibits immortalized human meibomian gland epithelial cell proliferation. (A) 13-*cis* RA at 2  $\mu$ M significantly inhibited cell proliferation within 2 days. (B) 13-*cis* RA showed dose-dependent inhibition of meibomian gland cell proliferation after 4 days in early- and late-passage cells. (C) Dose-dependent inhibition after 4 days was confirmed by WST-1 assay. Cells were cultured in KSFM containing 5 ng/mL EGF and 50  $\mu$ g/mL BPE. (A, B) 20,000 cells per well were plated in triplicate in 12-well plates. (C) 1350 cells per well were plated in 96-well plates with 8 wells/group. \* $P < 0.05$  compared with untreated control. Two-way ANOVA was used for (A), which showed a significant effect by RA; then Student's *t*-test was used to compare RA versus control at each time point. One-way ANOVA with Tukey post hoc method was used for (B, C).

incubated in renaturation buffer (5% 1 M Tris, 1% 0.5 M CaCl<sub>2</sub>, 2.5% Triton X-100) overnight at room temperature, then in development buffer (5% 1 M Tris, 1% 0.5 M CaCl<sub>2</sub>) for 24 hours at 37°C. Finally, gels were stained in buffer containing 40% methanol, 10% acetic acid, 0.5% Coomassie Blue dye. MMP activity was visible as clear bands against blue background.

### Statistical Analyses

One-way ANOVA, two-way ANOVA, and Student's *t*-test were performed using commercial software (Prism 5; GraphPad Software, Inc., La Jolla, CA). Fisher's PLSD was used as a post hoc test for one-way ANOVA (StatView512+; Abacus Corporation, Canoga Park, CA). For all tests, statistical significance was considered to be  $P < 0.05$ .

## RESULTS

### Effect of 13-*cis* RA on the Proliferation of Human Meibomian Gland Epithelial Cells

To determine the effect of 13-*cis* RA on meibomian gland cell proliferation, we performed both time course and dose-response studies. We also examined whether possible 13-*cis* RA influence was unique to these cells, or represented a general toxic effect on other cell types (e.g., human conjunctival epithelial cells).

At a concentration of 2  $\mu$ M, 13-*cis* RA significantly inhibited cell proliferation after 2, 3, and 4 days of treatment (Fig. 1A).

Moreover, meibomian gland epithelial cells at both early and late passages showed a dose-dependent decrease in cell number after 4 days of treatment with 1, 2, 5, and 10  $\mu$ M 13-*cis* RA (Fig. 1B). In fact, no countable cells were observed in wells exposed to 5 or 10  $\mu$ M 13-*cis* RA, and only rounded, poorly adherent cells remained (Fig. 2A). This dose-dependent decrease in cell number was also confirmed by WST-1 assay, a colorimetric assay based on the reduction of the tetrazolium salt WST-1 by mitochondrial dehydrogenase in viable cells (Fig. 1C).

The meibomian gland epithelial cells appeared to be more sensitive to 13-*cis* RA than other cell types such as conjunctival cells, whose proliferation was not inhibited by 1  $\mu$ M 13-*cis* RA (Fig. 2B), and whose cell morphology remained unchanged with up to 5  $\mu$ M 13-*cis* RA treatment (Fig. 2A). However, conjunctival epithelial cell morphology was altered by exposure to the high dose of 13-*cis* RA (i.e., 10  $\mu$ M), and appeared similar to that of meibomian gland epithelial cells (Fig. 2A).

### Influence of 13-*cis* RA on Cell Death

To assess the influence of 13-*cis* RA on apoptosis, human meibomian gland epithelial cells were treated with vehicle, 1, 2, or 5  $\mu$ M 13-*cis* RA, and then processed for TUNEL staining. We observed more TUNEL-positive cells in the 13-*cis* RA-treated condition (Fig. 3A). To quantify the cell death event, we stained cells treated with vehicle, 0.1, 1, or 2  $\mu$ M RA for 24 hours with FITC dye-conjugated Annexin V, which specifically binds to phosphatidylserine that translocates from the inner membrane leaflet to the outer membrane surface in the early

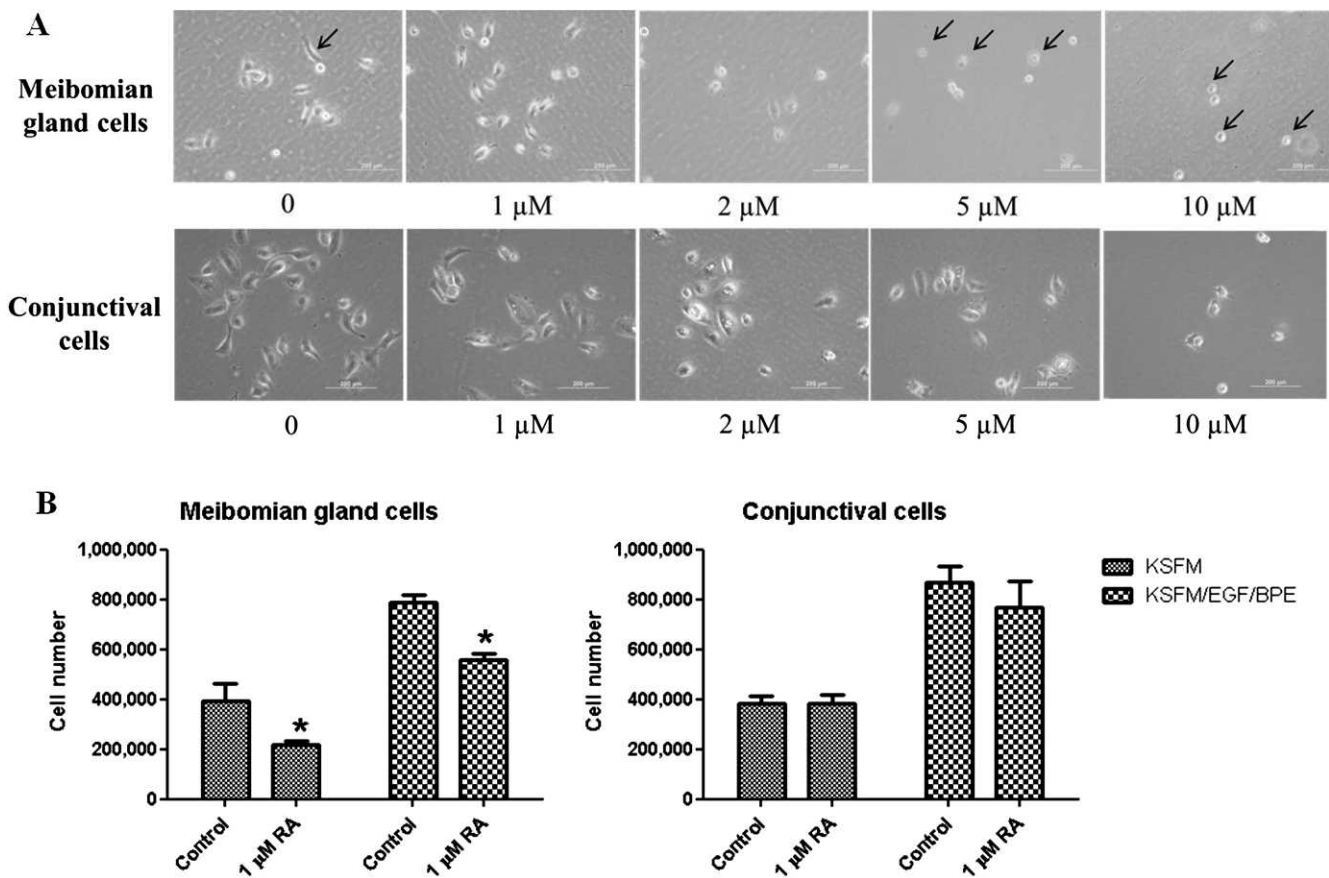


**FIGURE 2.** 13-*cis* RA inhibits proliferation of immortalized human meibomian gland epithelial cells, but not conjunctival epithelial cells, at low doses. **(A)** Morphology of meibomian gland and conjunctival epithelial cells after 1 day of treatment with various doses of RA. *Arrows* point to typical meibomian gland cells in control (normal), 5, and 10  $\mu$ M RA-treated (shrunken) conditions. *Scale bar*: 200  $\mu$ m. **(B)** Proliferation of meibomian gland epithelial cells, but not conjunctival epithelial cells, was inhibited after 5 days of treatment; 40,000 cells were plated per well in triplicates in six-well plates and treated with 1  $\mu$ M 13-*cis* RA or vehicle for 5 days. Student's *t*-test was used to compare between treatment conditions within each medium condition. \* $P < 0.05$ , compared with control.

event of apoptosis; and propidium iodide (PI), which binds to DNA in cells with compromised membranes (during late apoptosis or necrosis, where cells show early membrane permeabilization). Cells were sorted by flow cytometry and positive cells classified into early apoptosis (Annexin V positive, PI negative) or late apoptosis/necrosis (Annexin V and PI positive) groups. We observed a dose-dependent increase in the percentage of cells in late apoptosis/necrosis after 24 hours of treatment with 13-*cis* RA (Fig. 3B). In contrast, we did not observe any difference in early apoptosis events in cells treated for 4 hours (data not shown). As control experiments, staurosporin and hydrogen peroxide were used to induce apoptosis and necrosis, respectively. Staurosporin treatment (1  $\mu$ M, 3 hours) increased the percentage of cells in early apoptosis but not in late apoptosis/necrosis (Fig. 3C). By contrast, 0.5 mM hydrogen peroxide treatment for 3 hours increased the prevalence of both early apoptosis and late apoptosis/necrosis; after 24 hours, the percentage of cells in both groups was further increased, with a greater increase in late apoptosis/necrosis (Fig. 3C).

### Influence of 13-*cis* RA on Gene Expression in Human Meibomian Gland Epithelial Cells

To assess whether 13-*cis* RA alters gene expression in human meibomian gland cells, we treated cells with vehicle or 2  $\mu$ M

13-*cis* RA for 4 days ( $n = 3$ /group) and then processed the RNA for evaluation (Expression BeadChips; Illumina, and GeneSifter.net software; Geospiza). We chose these conditions based on the pronounced proliferation phenotype we had observed previously (Fig. 1A).

Our analysis demonstrated that 13-*cis* RA significantly ( $P < 0.05$ ) altered the expression of thousands of genes (3520  $\uparrow$ ; 3206  $\downarrow$ ) in human meibomian gland epithelial cells. As shown in Table 1, these included an upregulation of genes for various inflammatory mediators (e.g., IL-36 $\gamma$ , IL-15, IL-8, and IL-1 $\beta$ ) and proteases (e.g., matrix metalloproteinase 9 [MMP-9]), and a downregulation of genes for tyrosine kinase signaling (e.g., nerve growth factor b) and cell division (e.g., cell division cycle 25 homolog C).

Exposure to 13-*cis* RA had a marked effect on many Kyoto Encyclopedia of Genes and Genomes (KEGG) pathways, biological processes, molecular functions, and cellular components in human meibomian gland epithelial cells. As demonstrated in Table 2, 13-*cis* RA enhanced the expression of genes related to lysosomes, mitogen-activated protein kinase signaling, apoptosis, cell death, and lytic vacuoles. 13-*cis* RA also upregulated the activity of six genes associated with keratinization (e.g., small proline-rich proteins SPRRs 2F, 2D, and 1B). Conversely, 13-*cis* RA suppressed genes in processes linked to DNA replication, cell cycle, RNA transport and binding, and mitochondria.

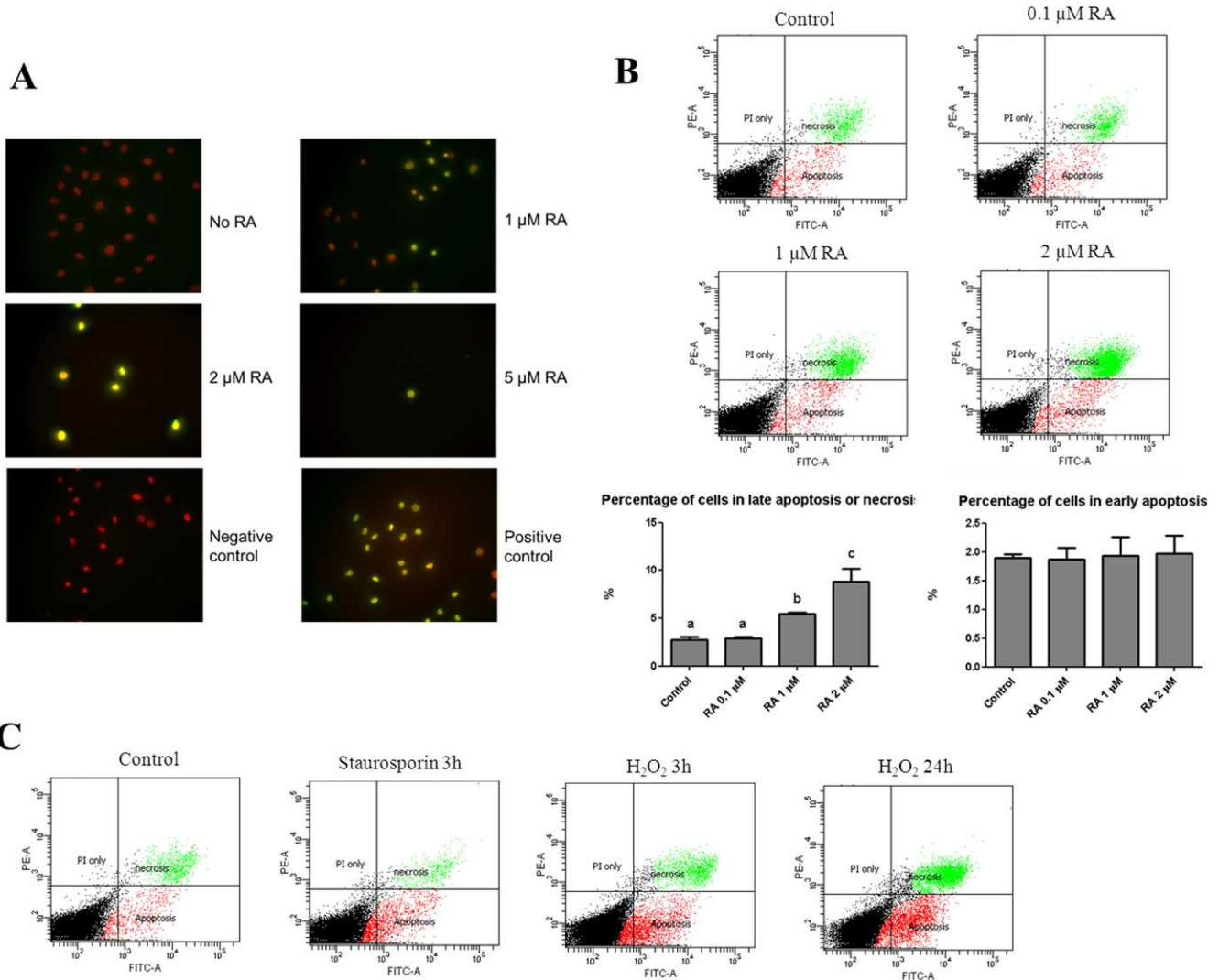


**FIGURE 3.** 13-*cis* RA induces cell death in immortalized human meibomian gland epithelial cells. **(A)** TUNEL staining of meibomian gland epithelial cells treated with various doses of RA for 4 days. Cells were stained with DAPI (red) for DNA and TUNEL (green) for the presence of nicked DNA ends. The negative control shows cells stained with only the labeled dUTP without the deoxynucleotidyl transferase; positive control cells were treated with DNase I prior to TUNEL staining. **(B)** Annexin V/PI flow cytometric analysis of meibomian gland cells treated with various doses of 13-*cis* RA for 24 hours. Cells (wells in triplicate) were cultured in KSFM containing EGF and BPE and treated with vehicle or 13-*cis* RA for 24 hours. Early apoptosis was defined as Annexin V positive, PI negative; late apoptosis or necrosis was defined as positive for both Annexin V and PI. Representative scatter dot graphs are shown in the top panel, and quantification in the bottom panel. One-way ANOVA followed by Fisher's PLSD post hoc test were used to determine significance ( $P < 0.05$ ), and different letters denote significant ( $P < 0.05$ ) differences among the groups. **(C)** Representative scatter dot graphs of control and agents known to induce apoptosis (staurosporin) and necrosis (H<sub>2</sub>O<sub>2</sub>).

### Effect of 13-*cis* RA on IL-1β and MMP-9 Protein Levels in Human Meibomian Gland Epithelial Cells

Our finding that 13-*cis* RA upregulated the expression of IL-1β and MMP-9 genes was of particular interest, given that these proteins have been linked to the development of dry eye disease.<sup>4</sup> Consequently, we sought to determine whether these augmented transcript levels are translated into heightened inflammatory and protease protein content.

As shown in Figure 4, treatment of human meibomian gland epithelial cells with 13-*cis* RA led to a significant increase in the levels of pro-IL-1β, IL-1β, and MMP-9 proteins in cell lysates (Fig. 4A). This effect was noticeable as early as 2 hours after 13-*cis* RA exposure. In addition, we observed elevated MMP-9 activity (Fig. 4B) and increased accumulation of pro-IL-1β (Fig. 4C) in supernatants of 13-*cis* RA-treated cells.

### Impact of 13-*cis* RA on AKT Signaling

To test our hypothesis that 13-*cis* RA reduces the activity of cell survival mediators, we explored whether this RA metabolite decreases phosphoinositide 3-kinase (PI3K)-protein kinase B (AKT) signaling. Such a signal, as indicated by AKT phosphorylation, promotes cell growth, proliferation, and survival.<sup>16</sup> In addition, AKT is a component of the phosphatidylinositol (PI) signaling system, which was significantly influenced by 13-*cis* RA (Table 2).

We discovered that 13-*cis* RA caused a significant, time-dependent decrease in the levels of phosphorylated AKT. This effect, as evidenced by a reduction in the phosphorylated, 60-kDa AKT band, began at 8 hours, and lasted at least until 24 hours, after treatment (Fig. 4A). 13-*cis* RA also increased the expression of another phosphorylated band, which migrated at approximately 50 kDa (Fig. 4A). This second band, which was

**TABLE 1.** Influence of 13-*cis* RA on Gene Expression in Immortalized Human Meibomian Gland Epithelial Cells

Accession Number	Gene	Ratio	P Value	Ontology
<b>13-<i>cis</i> RA &gt; placebo</b>				
NM_019618	Interleukin 36, $\gamma$	177.06	0.0002	Cell-cell signaling
NM_005328	Hyaluronan synthase 2	106.06	0.0008	Hyaluronan synthase activity
NM_001039966	G protein-coupled estrogen receptor 1	42.92	0.0002	G-protein coupled receptor protein signaling pathway
NM_172174	Interleukin 15	10.73	0.0001	NK T-cell proliferation
NM_005564	Lipocalin 2	8.98	0.0000	Ion transport
NM_001013398	Insulin-like growth factor binding protein 3	8.4	0.0010	Regulation of cell growth
NM_004994	Matrix metalloproteinase 9	8.11	0.0000	Proteolysis
NM_000584	Interleukin 8	7.29	0.0000	Angiogenesis
NM_139314	Angiopoietin-like 4	6.32	0.0000	Signal transduction
NM_000576	Interleukin-1 $\beta$	3.11	0.0004	Activation of MAPK activity
<b>Placebo &gt; 13-<i>cis</i> RA</b>				
NM_000782	Cytochrome P450, family 24, subfamily A, polypeptide 1	70,126.96	0.0010	Steroid metabolic process
NM_002506	Nerve growth factor ( $\beta$ polypeptide)	66,907.97	0.0023	Activation of MAPKK activity
NM_016240	Scavenger receptor class A, member 3	24.08	0.0002	Response to oxidative stress
NM_001442	Fatty acid binding protein 4, adipocyte	8.32	0.0011	Lipid metabolic process
NM_022809	Cell division cycle 25 homolog C	7.15	0.0001	Cell cycle checkpoint
NM_005879	TRAF interacting protein	6.92	0.0068	Induction of apoptosis
NM_006027	Exonuclease 1	6.67	0.0021	Meiosis
NM_001002876	Centromere protein M	6.62	0.0008	M phase of mitotic cell cycle
NM_018365	Meiosis-specific nuclear structural 1	5.91	0.0000	Meiosis
NM_006169	Nicotinamide <i>N</i> -methyltransferase	5.68	0.0076	Xenobiotic metabolic process

Relative ratios were calculated by comparing the degree of gene expression from vehicle- and 13-*cis* RA-treated human meibomian gland epithelial cells. Selected genes had a comparative *P* value (between treatments) of <0.05 and a known identity.

not seen in SaOS-2 osteosarcoma and LNCaP prostate cancer cells (data not shown), is in the molecular mass range for a caspase-cleaved AKT fragment.<sup>17,18</sup>

## DISCUSSION

Vitamin A plays a wide range of roles in cell proliferation, differentiation, apoptosis, and organ development.<sup>19</sup> However, active vitamin A metabolites, such as 13-*cis* RA, may also be toxic. 13-*cis* RA is the key ingredient of isotretinoin (Accutane), a drug used to treat acne, as well as in cosmetics advertised to reduce wrinkles and delay the appearance of aging. Unfortunately, 13-*cis* RA can have serious adverse effects on the meibomian gland, leading to ductal keratinization and obstruction, gland atrophy, gland drop out, and poor quality of meibomian gland secretions (i.e., meibum).<sup>1,20</sup> These signs are the hallmarks of MGD, a major cause of dry eye disease. In this study, we have started to address the mechanism of 13-*cis* RA-induced MGD at the cellular level, including inhibition of cell proliferation, promotion of cell death, alteration of gene expression, induction of the inflammatory mediators IL-1 $\beta$  and MMP-9, and reduced activation of the survival/proliferation signal AKT.

Our microarray data from human meibomian gland epithelial cells show that expression of genes related to proliferation decreases, and of those associated with cell death increases, in response to treatment with 13-*cis* RA. We confirmed these effects using proliferation assays and cell death analyses. 13-*cis* RA is known to inhibit proliferation and induce apoptosis in sebaceous gland cells.<sup>8</sup> Further, it is used as an antitumor drug in the treatment of various cancer types, including acute promyelocytic leukemia, head and neck squamous cell carcinoma, ovarian carcinoma, bladder cancer, and neuroblastoma.<sup>21</sup> However, the mechanisms of cell cycle arrest and cell death induction remain an important question. It has been shown that 13-*cis* RA-induced growth arrest in

MCF-7 cells involves reduced PI3K/AKT signaling.<sup>22</sup> The PI3K/AKT pathway is an important regulator of cell cycle progression and cell survival. 13-*cis* RA reduced phosphorylated AKT in human meibomian gland epithelial cells within 8 hours, and the signal remained suppressed for as long as 24 hours, with continuous treatment. 13-*cis* RA also stimulated the expression of a lower molecular weight, immunoreactive AKT species, which appears to be analogous to that following caspase-induced AKT cleavage.<sup>17,18</sup> We believe that suppression of the AKT pathway may be one of the primary mechanisms by which 13-*cis* RA inhibits proliferation and induces cell death in meibomian gland epithelial cells.

As to the mode of cell death, by staining cells with Annexin V and PI, and sorting by flow cytometry, we found that 13-*cis* RA induces a significant number of cells to enter late apoptosis/necrosis, but not early apoptosis (Fig. 3B). Interestingly, using the same Annexin V/PI technique to assay sebaceous gland cells treated with 13-*cis* RA, Nelson et al.<sup>8</sup> identified an increase in late apoptosis without any change in the prevalence of early apoptosis. This assay cannot differentiate between late apoptosis and necrosis, and thus 13-*cis* RA may increase apoptosis or necrosis. However, in our data, the similar percentage of cells undergoing early apoptosis, regardless of dose or length of exposure to 13-*cis* RA, suggests that 13-*cis* RA may induce necrosis, rather than apoptosis, in meibomian gland cells. Further, control experiments using staurosporin and hydrogen peroxide demonstrated that immortalized meibomian gland cells are capable of undergoing both apoptosis and necrosis. This conclusion does not contradict our TUNEL assay results, because TUNEL, which detects nicked DNA ends, stains both necrotic and apoptotic cells.<sup>23</sup> Recently it has been recognized that, similar to apoptosis, necrosis is also a type of programmed cell death,<sup>24</sup> and it is regulated by cellular machinery composed of an increasing list of factors.<sup>25</sup> The mechanism of necrosis

TABLE 2. Effect of 13-*cis* RA on Gene Ontologies in Human Meibomian Gland Epithelial Cells

KEGG/Ontologies	RA Genes ↑	PI Genes ↑	RA z-Score	PI z-Score
KEGG pathway				
Lysosome	40	8	<b>5.88</b>	-2.61
Phosphatidylinositol signaling system	25	6	<b>4.45</b>	-1.82
Phagosome	39	11	<b>4.12</b>	-2.64
Endocytosis	48	17	<b>3.91</b>	-2.62
Ubiquitin-mediated proteolysis	34	29	<b>3.59</b>	2.14
Glycerophospholipid metabolism	21	7	<b>3.22</b>	-1.46
Apoptosis	23	8	<b>3.14</b>	-1.56
Focal adhesion	44	21	<b>3.13</b>	-1.79
MAPK signaling pathway	53	20	<b>2.57</b>	-3.52
Jak-STAT signaling pathway	32	8	<b>2.26</b>	-3.45
DNA replication	1	29	-1.96	<b>11.28</b>
Cell cycle	13	56	-1.24	<b>9.59</b>
RNA transport	7	64	-3.52	<b>9.42</b>
Spliceosome	6	53	-3.1	<b>8.68</b>
Metabolic pathways	152	251	-0.4	<b>8.42</b>
Nucleotide excision repair	3	22	-1.4	<b>6.67</b>
Pyrimidine metabolism	17	36	0.96	<b>6.3</b>
Purine metabolism	19	50	-0.85	<b>6</b>
Proteasome	1	20	-2.31	<b>5.68</b>
Oxidative phosphorylation	13	38	-1.11	<b>5.23</b>
Biological process				
Protein localization	248	170	<b>7.15</b>	1.63
Regulation of signal transduction	272	116	<b>6.82</b>	-4.91
Protein transport	206	131	<b>6.75</b>	0.68
Regulation of response to stimulus	340	155	<b>6.5</b>	-5.64
Cell death	274	208	<b>5.28</b>	1.51
Apoptosis	250	197	<b>5.04</b>	2.08
Cell cycle phase	86	278	-2.14	<b>20.33</b>
Mitotic cell cycle	78	257	-2.04	<b>19.88</b>
Cell cycle process	110	309	-1.78	<b>19.69</b>
Cell cycle	160	354	-0.82	<b>17.96</b>
Gene expression	449	545	-1.22	<b>6.8</b>
Cell differentiation	327	192	1.92	-5.71
Molecular functions				
Protein binding	1159	1109	<b>7.01</b>	9.62
Ubiquitin-protein ligase activity	57	27	<b>4.91</b>	-0.32
Phospholipid binding	52	17	<b>4.81</b>	-1.86
Protein kinase binding	52	32	<b>4.6</b>	1.18
Kinase binding	59	41	<b>4.57</b>	1.92
Lipid binding	87	40	<b>3.32</b>	-2.45
RNA binding	71	229	-4.45	<b>13.74</b>
Structural constituent of ribosome	7	66	-3.55	<b>10.92</b>
Transferase activity, transferring one-carbon groups	15	56	-2.44	<b>7.05</b>
Nucleic acid binding	384	508	-3.75	<b>6.11</b>
Nuclease activity	22	46	-0.25	<b>5.94</b>
Oxidoreductase activity	94	138	-0.46	<b>5.75</b>
Cellular components				
Endosome	121	33	<b>8.1</b>	-3.17
Vacuole	96	23	<b>8.07</b>	-2.92
Cytoplasm	1334	1342	<b>7.58</b>	15.53
Lysosome	79	22	<b>7</b>	-2.22
Lytic vacuole	79	22	<b>7</b>	-2.22
Golgi apparatus	208	77	<b>6.64</b>	-4.36
Intracellular organelle lumen	338	653	-2.04	<b>21.37</b>
Nuclear part	336	610	-1.23	<b>19.81</b>
Mitochondrion	164	386	-1.88	<b>19.52</b>
Ribonucleoprotein complex	37	203	-4.6	<b>19.08</b>

TABLE 2. Continued

KEGG/Ontologies	RA Genes ↑	PI Genes ↑	RA z-Score	PI z-Score
Macromolecular complex	427	733	<b>-3.23</b>	<b>18.13</b>
Nuclear lumen	297	524	-1.15	17.36

A z-score is a statistical rating of the relative expression of genes, and depicts over- or underrepresentation in a given gene list.<sup>41</sup> Positive z-scores reflect gene ontology terms with a greater number of genes meeting the criterion than is expected by chance, whereas negative z-scores represent fewer genes meeting the criterion than expected by chance; z-scores with values > 2.0 or less than -2.0 are significant. High and low values for the placebo (PI) and 13-*cis* RA (RA) groups in specific ontologies are highlighted in *bold print*. RA Genes ↑, number of genes upregulated in 13-*cis* RA-treated meibomian gland epithelial cells, as compared with those of the “placebo” group; PI Genes ↑, number of genes upregulated in the placebo-treated meibomian gland epithelial cells, as compared with those of the “RA” group; z-score, specific score for the upregulated gene ontology in the placebo- and 13-*cis* RA-exposed human meibomian gland epithelial cells.

regulated by 13-*cis* RA will be an interesting subject for future studies.

13-*cis* RA significantly increased the expression of a variety of genes encoding inflammatory mediators, including IL-1 $\beta$ , IL-8, IL-15, and IL-36 $\gamma$  in human meibomian gland epithelial cells. These cytokines, which serve as chemoattractants, Jak kinase and NF- $\kappa$ B activators, and/or regulators of leukocyte function<sup>26</sup> (<http://www.genecards.org>), could theoretically promote extravasation of immune cells into the adjacent conjunctiva in vivo. Such conjunctival inflammation, termed blepharitis, may occur during MGD.<sup>27,28</sup> 13-*cis* RA also upregulated the transcription and translation of MMP-9 and IL-1 $\beta$ , both of which have been implicated in the pathophysiology of dry eye disease.<sup>4,29,30</sup>

In addition to their roles as inflammatory mediators at the ocular surface, IL-1 $\beta$  and MMP-9 are also involved in regulation of cell death. For example, IL-1 $\beta$  promotes pancreatic epithelial cell death by inducing endoplasmic reticulum stress and activating c-Jun NH(2)-terminal protein kinase (JNK).<sup>31</sup> Interestingly, our microarray data show that the JNK cascade is upregulated by 13-*cis* RA (Table 1). MMP-9 promotes cell death and inhibits cell proliferation in cultured human keratino-

cytes<sup>32</sup> and MMP-9 deficiency protects against retinal ganglion cell death.<sup>33</sup> Thus, it is possible that 13-*cis* RA promotes meibomian gland epithelial cell death, in part, via IL-1 $\beta$  and MMP-9. This hypothesis needs to be addressed in future studies.

13-*cis* RA significantly enhanced the expression of genes encoding SPRRs 1B, 2D, and 2F in human meibomian gland epithelial cells. Similarly, we have previously found that the levels of SPRR mRNAs (e.g., 2A, 2E, 2F, and 3) are significantly increased in meibomian glands from patients with MGD.<sup>14</sup> If translated, it is possible that such upregulated SPRRs may be responsible, at least in part, for the hyperkeratinization of meibomian gland ductal epithelium in MGD. The reason is that SPRRs are known to promote keratinization,<sup>34-38</sup> and this process is believed to be a primary cause of MGD.<sup>1,39,40</sup>

In conclusion, at the outset of this study, we hypothesized that 13-*cis* RA alters meibomian gland epithelial cell gene expression, reduces the activity of cell survival mediators, inhibits proliferation, and induces meibocyte cell death. Our findings support our hypotheses, and suggest that 13-*cis* RA may act on the meibomian gland in a manner analogous to that of the sebaceous gland.

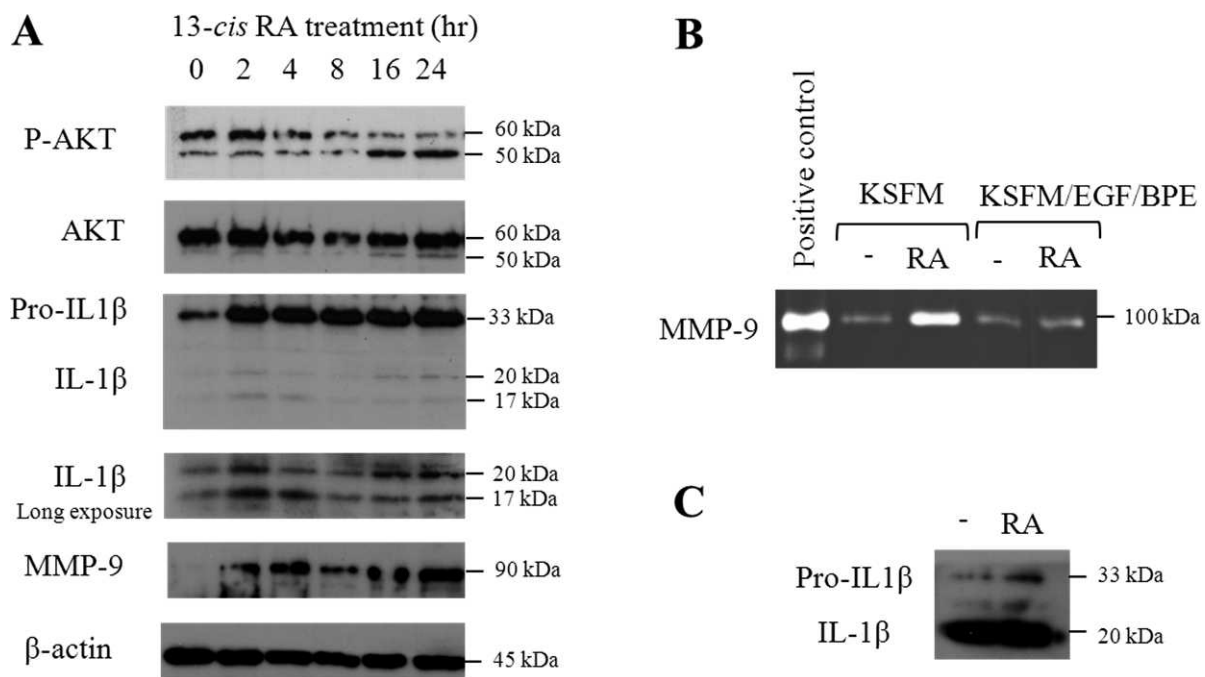


FIGURE 4. 13-*cis* RA induces alterations in protein content and activity in immortalized human meibomian gland epithelial cells. (A) Immunoblot images showing changes in p-AKT, IL-1 $\beta$ , and MMP-9 in cell lysates in response to 1  $\mu$ M 13-*cis* RA. (B) Zymography image of MMP-9 in the culture medium after 13-*cis* RA treatment. (C) Immunoblot image of IL-1 $\beta$  secreted into culture medium after 13-*cis* RA treatment. (B, C) Cells were treated with 1  $\mu$ M 13-*cis* RA for 24 hours.



## Acknowledgments

The authors thank Yueran Yan for his assistance of preserving 13-*cis* retinoic acid in argon gas.

Supported by National Eye Institute/National Institutes of Health Grant R01 EY05612; the Margaret S. Sinon Scholar in Ocular Surface Research and the AFER/Vistakon Dry Eye Fellowship. The authors alone are responsible for the content and writing of the paper.

Disclosure: **J. Ding**, None; **W.R. Kam**, None; **J. Dieckow**, None; **D.A. Sullivan**, None

## References

- Knop E, Knop N, Millar T, Obata H, Sullivan DA. The International Workshop on Meibomian Gland Dysfunction: report of the subcommittee on anatomy, physiology, and pathophysiology of the meibomian gland. *Invest Ophthalmol Vis Sci*. 2011;52:1938-1978.
- Green-Church KB, Butovich I, Willcox M, et al. The International Workshop on Meibomian Gland Dysfunction: report of the subcommittee on tear film lipids and lipid-protein interactions in health and disease. *Invest Ophthalmol Vis Sci*. 2011;52:1979-1993.
- Nelson JD, Shimazaki J, Benitez-del-Castillo JM, et al. The International Workshop on Meibomian Gland Dysfunction: report of the definition and classification subcommittee. *Invest Ophthalmol Vis Sci*. 2011;52:1930-1937.
- The epidemiology of dry eye disease: report of the Epidemiology Subcommittee of the International Dry Eye WorkShop. *Ocul Surf*. 2007;5:93-107.
- Viso E, Gude F, Rodriguez-Ares MT. The association of meibomian gland dysfunction and other common ocular diseases with dry eye: a population-based study in Spain. *Cornea*. 2011;30:1-6.
- Schaumberg DA, Nichols JJ, Papas EB, Tong L, Uchino M, Nichols KK. The International Workshop on Meibomian Gland Dysfunction: report of the subcommittee on the epidemiology of, and associated risk factors for, MGD. *Invest Ophthalmol Vis Sci*. 2011;52:1994-2005.
- Zouboulis CC. Isotretinoin revisited: pluripotent effects on human sebaceous gland cells. *J Invest Dermatol*. 2006;126:2154-2156.
- Nelson AM, Gilliland KL, Cong Z, Thiboutot DM. 13-*cis* Retinoic acid induces apoptosis and cell cycle arrest in human SEB-1 sebocytes. *J Invest Dermatol*. 2006;126:2178-2189.
- Tsukada M, Schroder M, Roos TC, et al. 13-*cis* Retinoic acid exerts its specific activity on human sebocytes through selective intracellular isomerization to all-*trans* retinoic acid and binding to retinoid acid receptors. *J Invest Dermatol*. 2000;115:321-327.
- Schaumberg DA, Sullivan DA, Buring JE, Dana MR. Prevalence of dry eye syndrome among US women. *Am J Ophthalmol*. 2003;136:318-326.
- Nelson AM, Zhao W, Gilliland KL, Zaenglein AL, Liu W, Thiboutot DM. Neutrophil gelatinase-associated lipocalin mediates 13-*cis* retinoic acid-induced apoptosis of human sebaceous gland cells. *J Clin Invest*. 2008;118:1468-1478.
- Liu S, Hatton MP, Khandelwal P, Sullivan DA. Culture, immortalization, and characterization of human meibomian gland epithelial cells. *Invest Ophthalmol Vis Sci*. 2010;51:3993-4005.
- Kam WR, Sullivan DA. Neurotransmitter influence on human meibomian gland epithelial cells. *Invest Ophthalmol Vis Sci*. 2011;52:8543-8548.
- Liu S, Richards SM, Lo K, Hatton M, Fay A, Sullivan DA. Changes in gene expression in human meibomian gland dysfunction. *Invest Ophthalmol Vis Sci*. 2011;52:2727-2740.
- Shi L, Reid LH, Jones WD, et al. The MicroArray Quality Control (MAQC) project shows inter- and intraplatform reproducibility of gene expression measurements. *Nat Biotechnol*. 2006;24:1151-1161.
- Song G, Ouyang G, Bao S. The activation of Akt/PKB signaling pathway and cell survival. *J Cell Mol Med*. 2005;9:59-71.
- Medina EA, Afsari RR, Ravid T, Castillo SS, Erickson KL, Goldkorn T. Tumor necrosis factor- $\alpha$  decreases Akt protein levels in 3T3-L1 adipocytes via the caspase-dependent ubiquitination of Akt. *Endocrinology*. 2005;146:2726-2735.
- Rokudai S, Fujita N, Hashimoto Y, Tsuruo T. Cleavage and inactivation of antiapoptotic Akt/PKB by caspases during apoptosis. *J Cell Physiol*. 2000;182:290-296.
- Gutierrez-Mazariegos J, Theodosiou M, Campo-Paysaa F, Schubert M. Vitamin A: a multifunctional tool for development. *Semin Cell Dev Biol*. 2011;22:603-610.
- Lambert RW, Smith RE. Effects of 13-*cis*-retinoic acid on the hamster meibomian gland. *J Invest Dermatol*. 1989;92:321-325.
- Siddikuzzaman, Guruvayoorappan C, Berlin Grace VM. All-trans retinoic acid and cancer. *Immunopharmacol Immunotoxicol*. 2011;33:241-249.
- del Rincon SV, Rousseau C, Samanta R, Miller WH Jr. Retinoic acid-induced growth arrest of MCF-7 cells involves the selective regulation of the IRS-1/PI 3-kinase/AKT pathway. *Oncogene*. 2003;22:3353-3360.
- Grasl-Kraupp B, Ruttkay-Nedecky B, Koudelka H, Bukowska K, Bursch W, Schulte-Hermann R. In situ detection of fragmented DNA (TUNEL assay) fails to discriminate among apoptosis, necrosis, and autolytic cell death: a cautionary note. *Hepatology*. 1995;21:1465-1468.
- Duprez L, Wirawan E, Vanden Berghe T, Vandenabeele P. Major cell death pathways at a glance. *Microbes Infect*. 2009;11:1050-1062.
- Hitomi J, Christofferson DE, Ng A, et al. Identification of a molecular signaling network that regulates a cellular necrotic cell death pathway. *Cell*. 2008;135:1311-1323.
- Safran M, Dalah I, Alexander J, et al. GeneCards Version 3: the human gene integrator [published online ahead of print August 5, 2010]. *Database (Oxford)*. doi:10.1093/database/baq020.
- Messmer EM, Torres Suarez E, Mackert MI, Zapp DM, Kampik A. [In vivo confocal microscopy in blepharitis]. *Klin Monatsbl Augenheilkd*. 2005;222:894-900.
- Matsumoto Y, Shigeno Y, Sato EA, et al. The evaluation of the treatment response in obstructive meibomian gland disease by in vivo laser confocal microscopy. *Graefes Arch Clin Exp Ophthalmol*. 2009;247:821-829.
- Solomon A, Dursun D, Liu Z, Xie Y, Macri A, Pflugfelder SC. Pro- and anti-inflammatory forms of interleukin-1 in the tear fluid and conjunctiva of patients with dry-eye disease. *Invest Ophthalmol Vis Sci*. 2001;42:2283-2292.
- Luo L, Li DQ, Doshi A, Farley W, Corrales RM, Pflugfelder SC. Experimental dry eye stimulates production of inflammatory cytokines and MMP-9 and activates MAPK signaling pathways on the ocular surface. *Invest Ophthalmol Vis Sci*. 2004;45:4293-4301.
- Verma G, Datta M. IL-1 $\beta$  induces ER stress in a JNK dependent manner that determines cell death in human pancreatic epithelial MIA PaCa-2 cells. *Apoptosis*. 2010;15:864-876.
- Xue M, Jackson CJ. Autocrine actions of matrix metalloproteinase (MMP)-2 counter the effects of MMP-9 to promote survival and prevent terminal differentiation of cultured human keratinocytes. *J Invest Dermatol*. 2008;128:2676-2685.
- Chintala SK, Zhang X, Austin JS, Fini ME. Deficiency in matrix metalloproteinase gelatinase B (MMP-9) protects against

- retinal ganglion cell death after optic nerve ligation. *J Biol Chem.* 2002;277:47461-47468.
34. Hohl D, de Viragh PA, Amiguet-Barras F, Gibbs S, Backendorf C, Huber M. The small proline-rich proteins constitute a multigene family of differentially regulated cornified cell envelope precursor proteins. *J Invest Dermatol.* 1995;104:902-909.
  35. Kawasaki S, Kawamoto S, Yokoi N, et al. Up-regulated gene expression in the conjunctival epithelium of patients with Sjogren's syndrome. *Exp Eye Res.* 2003;77:17-26.
  36. Li S, Gallup M, Chen YT, McNamara NA. Molecular mechanism of proinflammatory cytokine-mediated squamous metaplasia in human corneal epithelial cells. *Invest Ophthalmol Vis Sci.* 2010;51:2466-2475.
  37. Iizuka H, Takahashi H, Honma M, Ishida-Yamamoto A. Unique keratinization process in psoriasis: late differentiation markers are abolished because of the premature cell death. *J Dermatol.* 2004;31:271-276.
  38. Ishida-Yamamoto A, Iizuka H, Manabe M, et al. Altered distribution of keratinization markers in epidermolytic hyperkeratosis. *Arch Dermatol Res.* 1995;287:705-711.
  39. Obata H. Anatomy and histopathology of human meibomian gland. *Cornea.* 2002;21:S70-S74.
  40. Gutgesell VJ, Stern GA, Hood CI. Histopathology of meibomian gland dysfunction. *Am J Ophthalmol.* 1982;94:383-387.
  41. Doniger SW, Salomonis N, Dahlquist KD, Vranizan K, Lawlor SC, Conklin BR. MAPPFinder: using Gene Ontology and GenMAPP to create a global gene-expression profile from microarray data. *Genome Biol.* 2003;4:R7.